Primljen / Received: 1.4.2025.
Ispravljen / Corrected: 15.7.2025.
Prihvaćen / Accepted: 18.8.2025.
Dostupno online / Available online: 10.2.2026.

Mechanical properties of UHPFRC beam-column joints with high-strength stirrups

Author:

Prof. **Julin Wang**, PhD. CE
Shanxi Vocational University of Engineering Science and Technology, China
Faculty of Architectural Engineering
wangjl_tj@163.com
Corresponding author

Research Paper

Julin Wang

Mechanical properties of UHPFRC beam-column joints with high-strength stirrups

Reinforced concrete beam-column joints are prone to damage during severe earthquakes. Substituting normal concrete with ultra-high-performance fibre-reinforced concrete (UHPFRC), which has outstanding mechanical properties, can improve the earthquake resistance capacity of these joints. However, UHPFRC joints with ordinary-strength stirrups do not reduce the amount of transverse reinforcement, causing construction difficulties. This study investigates UHPFRC beam-column joints with high-strength stirrups and evaluates their mechanical properties under combined axial and cyclic lateral loads via a detailed experimental program. Four beam-column joint specimens were fabricated and tested. The joint core of one specimen was made of ordinary concrete and that of the other three was made of UHPFRC. The test parameters included the types of materials used, yield strength, and volumetric ratio of the stirrups. The experimental results demonstrated that high-strength stirrups restrained the shear deformation, effectively improved the ductility and energy dissipation of the joints, and reduced the amount of transverse reinforcement while maintaining the same seismic capacity.

Key words:
beam-column joints, ultra-high performance fibre-reinforced concrete, high-strength stirrups, mechanical properties, cyclic loading

Prethodno priopćenje

Julin Wang

Mehanička svojstva spojeva greda-stup od betona visokih uporabnih svojstava armiranog vlaknima (UHPFRC) s poprečnom armaturom visoke čvrstoće

Spojevi armiranobetonskih greda i stupova skloni su oštećenjima uslijed jakih potresa. Zamjena običnog betona betonom vrlo visokih uporabnih svojstava armiranog vlaknima (UHPFRC), koji ima izvanredna mehanička svojstva, može poboljšati otpornost ovih spojeva na potrese. Međutim, UHPFRC spojevi s poprečnom armaturom uobičajene čvrstoće ne smanjuju količinu poprečne armature, što može uzrokovati poteškoće pri izvedbi. Predmet su ovog istraživanja UHPFRC spojevi greda-stup ojačani poprečnom armaturom velike čvrstoće, pri čemu se njihova mehanička svojstva pri kombiniranom aksijalnom i cikličkom bočnom opterećenju procjenjuju eksperimentalnim ispitivanjima. Izrađena su i ispitana četiri uzorka spoja grede i stupa. Jezgra spoja jednog uzorka bila je izrađena od običnog betona, a preostala su tri uzorka imala jezgru izrađenu od UHPFRC-a. Ispitni parametri obuhvaćali su vrste primijenjenih materijala, granicu popuštanja te koeficijent armiranja poprečnom armaturom. Rezultati ispitivanja pokazali su da poprečna armatura visoke čvrstoće djelotvorno ograničava posmična naprezanja, povećava duktilnost i sposobnost raspršivanja energije spojeva te omogućuje smanjenje poprečne armature bez umanjenja seizmičke otpornosti.

Ključne riječi:
spojevi greda-stup, beton visoke čvrstoće armiran vlaknima, poprečna armatura visoke čvrstoće, mehanička svojstva, cikličko opterećenje

1. Introduction

The shear failure of beam-column joints has been identified as a primary reason for the collapse of frame buildings during severe earthquakes [1-10]. Therefore, enhancing the seismic performance of beam-column joints has attracted the attention of civil engineers.

Tiwary et al. [11] added diagonal crossbars to beam-column joints to enhance their seismic performance. Tang et al. [12] proposed an innovative concrete beam-column joint locally enhanced by ultra-high-performance concrete (UHPC) shells and tested full-scale specimens to investigate the seismic behaviours of novel joints. The experimental results revealed that concrete beam-column joints with UHPC shells behaved satisfactorily under low-cycle reversed loadings. Wang et al. [13] conducted quasi-static tests on nine different UHPFRC beam-column joints to investigate their seismic behaviour and shear-bearing capacity. Sarmiento et al. [14] fabricated and tested beam-column joint specimens under cyclic lateral loads and concluded that the UHPFRC joint specimens had 157% higher energy dissipation than ordinary concrete specimens. Annadurai and Ravichandran [15] demonstrated that UHPFRC beam-column joints extend excellent displacement ductility capacity. According to Tsonos et al. [16], UHPFRC beam-column joints exhibit satisfactory ductility. Abolfazl et al. [17] experimentally proved that the use of UHPFRC in beam-column joints enhances the load-carrying capacity of joints. Dehong et al. [18] reported that UHPFRC beam-column joints exhibit excellent seismic performance.

From the above literature, we can conclude that both the bearing capacity and deformation capacity of beam-column joints are improved when normal concrete is by substituted with UHPFRC. However, to enhance the shear resistance, more transverse steel bars must be arranged at the joints, which can cause construction difficulties. Several approaches have been proposed to solve this problem. A novel precast UHPFRC beam-column joint was developed, which reduced the amount of transverse reinforcement in the joints and simplified the construction process [19-22]. Shi et al. [23, 24] attempted to prevent reinforcement concentration and reduce the amount of transverse reinforcement in UHPFRC joints through the ideal usage of steel fibres. In [25], an analytical and experimental investigation into the cyclic load behaviour of beam-column joints was conducted; results indicated that the transverse reinforcement requirement for joints with steel fibres was lower than the Eurocode specifications. Abdo et al. [26] found that the presence of stirrups in a UHPFRC beam-column joint had little effect on its properties. Gupta et al. [27] conducted a series of tests and concluded that steel fibres effectively improve the shear-carrying capacity of joints with increased ductility and damage tolerance without the need for closely spaced stirrups in the joint hinge region.

Although several studies have focused on the role of steel fibres, few studies have been conducted on UHPFRC beam-column joints with high-strength stirrups. Accordingly, the mechanical properties of UHPFRC beam-column joints with high-strength stirrups were experimentally analysed in the study.

2. Experimental program

2.1. Specimen details

To investigate the mechanical properties of UHPFRC beam-column joints with high-strength stirrups, four joint specimens were designed and fabricated. Among these, one specimen was made of ordinary concrete and the other three were made of UHPFRC. The test specimens were labelled using the joint core material type and specimen number. For example, "RC1" refers to the specimen made of reinforced concrete and "UHPFRC2" refers to the second specimen made of UHPFRC.

All specimens had the same geometry and longitudinal reinforcement, as shown in Figure 1 and Table 1. The amount of longitudinal reinforcement in the beams and columns was determined according to the Code for the Design of Concrete Structures (GB 50010-2010) [28]. The ends of the columns and beams were points of contraflexure; that is, the bending moment is zero at the ends and its sign changes. The test variables included the types of materials used, yield strength, and volumetric ratio of the stirrups in the joint core. High-strength stirrups were used in the joint cores of UHPFRC2 and UHPFRC3, whereas the stirrups

Table 1. Reinforcement arrangement of specimens

Specimen	Longitudinal bars		Stirrups			
	Beams	**Columns**	**Beams** [mm]	**Columns** [mm]	**Joint cores** [mm]	**Volumetric ratio in joint cores** [%]
RC1	6Φ22	8Φ25	Φ8/90	Φ8/80	Φ8/120	0.92
UHPFRC1	6Φ22	8Φ25	Φ8/90	Φ8/80	Φ8/120	0.92
UHPFRC2	6Φ22	8Φ25	Φ8/90	Φ8/80	Φ5/100	0.92
UHPFRC3	6Φ22	8Φ25	Φ8/90	Φ8/80	Φ5/85	1.09

in the joint cores of RC1 and UHPFRC1 were of ordinary strength. The compressive cube strength of the concrete was 49.1MPa.

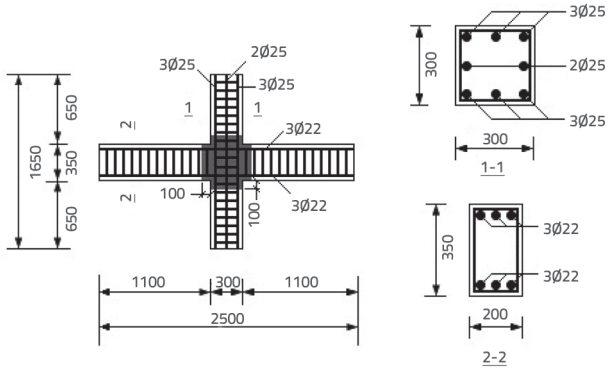

Figure 1. Specimen dimensions and reinforcement details (unit: mm)

2.2. Materials

The UHPFRC was composed of ordinary Portland cement, water, quartz sand, silica fume, a superplasticiser, steel fibre (13 mm in length with a diameter of 0.2 mm, and a yield strength of 1100 MPa). The mixture proportions and material properties of the UHPFRC are presented in Tables 2 and 3, respectively.

Screw-threaded steel bars of grade HRB400 were used for the longitudinal reinforcement of the beams and columns. The joint cores of RC1 and UHPFRC1 were equipped with ordinary strength stirrups of grade HRB335, whereas the joint cores of UHPFRC2 and UHPFRC3 had high-strength stirrups. The material properties of the steel bars are listed in Table 4, and the stress-strain curve of the high-strength stirrup is shown in Figure 2.

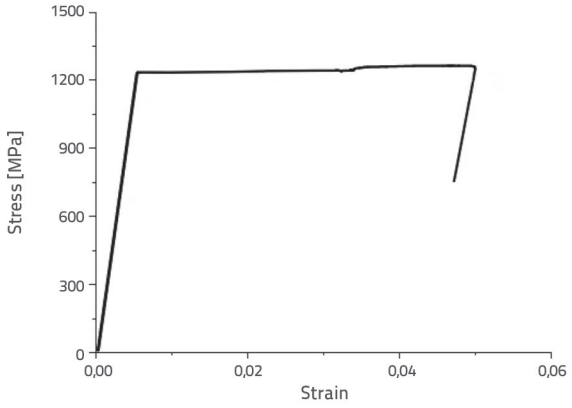

Figure 2. Stress-strain curves of the high-strength stirrups

2.3. Experimental setup and loading procedure

The experimental setup is shown in Figures 3(a) and 3(b). Pseudo-static tests were conducted using a material testing system (MTS); it consisted of a 2200 kN hydraulic jack positioned vertically at the top of the column to generate a constant compressive load, and an electro-hydraulic servo actuator was applied at the column end to produce cyclic lateral loading. The lower end of the column was attached to a strong floor using a steel hinge. The left and right ends of the beam were supported on a steel roll by using a connecting rod to allow rotation and free horizontal movement, respectively.

At the beginning of the experiment, a constant vertical load was applied to the top of the column; following this, a reversed cyclic horizontal load was applied by the actuator mounted on the reaction wall. A mixed scheme of load and displacement was adopted to apply the horizontal load. For load control, the amplitude of the load was increased by

Table 2. Mixture composition of UHPFRC for 1 m³

Ingredients	Cement	Water	Silica fume	Quartz sand	Superplasticizer	Steel fibers
Mass [kg]	900	165	216	1004	42	160

Table 3. Material properties of UHPFRC

Compressive strength [MPa]	**Tensile strength** [MPa]	**Ultimate tensile strain**	**Ultimate compressive strain**
109.5	7.4	0.0125	0.0038

Table 4. Mechanical properties of the steel bars

Species	Diameter [mm]	Yield strength [MPa]	Percentage elongation [%]	Elastic modulus [MPa]
HRB335	8.0	409	26.0	1.69×10^5
HRB400	22	448	37.1	1.86×10^5
	25	448	37.1	1.86×10^5
High-strength stirrups	5.0	1238	10.2	2.19×10^5

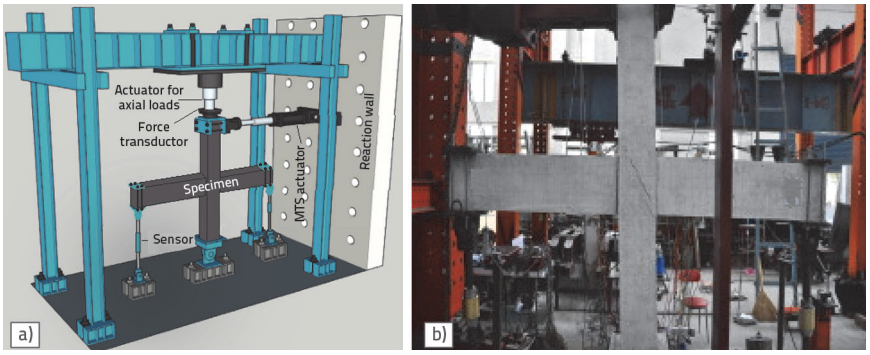

Figure 3. Experimental setup: a) schematic; b) site photo

10 kN per cycle until the specimens yielded. Subsequently, displacement control was applied, wherein the displacement increment was 0.15 times the yield displacement and two cycles were applied for each displacement level. The loading was terminated when the specimens were damaged or when their load-carrying capacity decreased to 85% of the ultimate load.

2.4. Layout of measurement pPoints

The arrangement of the monitoring points used in the experiment is shown in Figure 4.

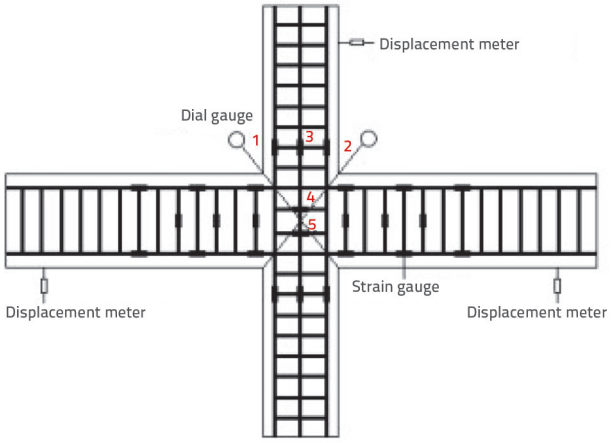

Figure 4. Monitoring device layout

Two crossing dial indicators were arranged at the joint core to measure shear deformations. Twenty-six strain gauges were placed on the reinforcement to investigate the steel strain (eight on the stirrups, twelve on the longitudinal bars of the beam, and six on the longitudinal bars of the column). A displacement meter was used to measure the horizontal displacement at the top of the column, and two displacement meters were placed at the left and right ends of the beam to measure the constraint reaction.

3. Results and discussion

3.1. Test phenomena

The failure modes of the four specimens under reverse cyclic loading were similar, and each specimen underwent four stages, cracking stage, yielding stage, ultimate stage, and failure stage. Figure 5 shows the failure modes of the four specimens, and Table 5 lists the loads and displacements during crack development.

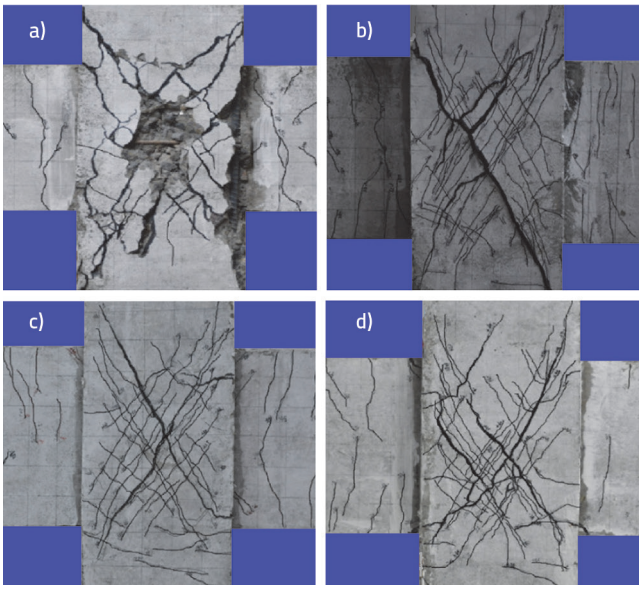

Figure 5. Failure modes of the specimens: a) RC1, b) UHPFRC1, c) UHPFRC2, d) UHPFRC3

Table 5. Loads and displacements in crack development process

Columns	The first crack occurred		X-shaped cross oblique crack appearing		Yielding	
	Displacement [mm]	**Load** [kN]	**Displacement** [mm]	**Load** [kN]	**Displacement** [mm]	**Load** [kN]
RC1	4	20	17	110	21	188
UHPFRC1	3	50	11	151	46	290
UHPFRC2	5	53	9	154	39	296
UHPFRC3	4	49	8	153	45	289

RC1 was composed of ordinary concrete with ordinary-strength stirrups in the joint core. When loaded to 20 kN, the first crack appeared on the tension side of the beam approximately 114 mm from the edge of the joint. As loading progressed, new cracks were created on the left and right sides of the first crack. When it was loaded to 110 kN, oblique cracks with a width of about 0.1 mm appeared near the diagonal intersection of the joint core. When the loading was increased to 160 kN, the X-shaped cross-oblique cracks became the main crack, and their width increased to 0.5 mm. The specimens were loaded with displacement control after yielding. When the displacement drift was increased to 5.6%, the bearing capacity reached 85% of the maximum load and the loading stopped. From the final failure mode (Figure 5(a)), it can be observed that the failure of RC1 was due to shear failure in the joint core.

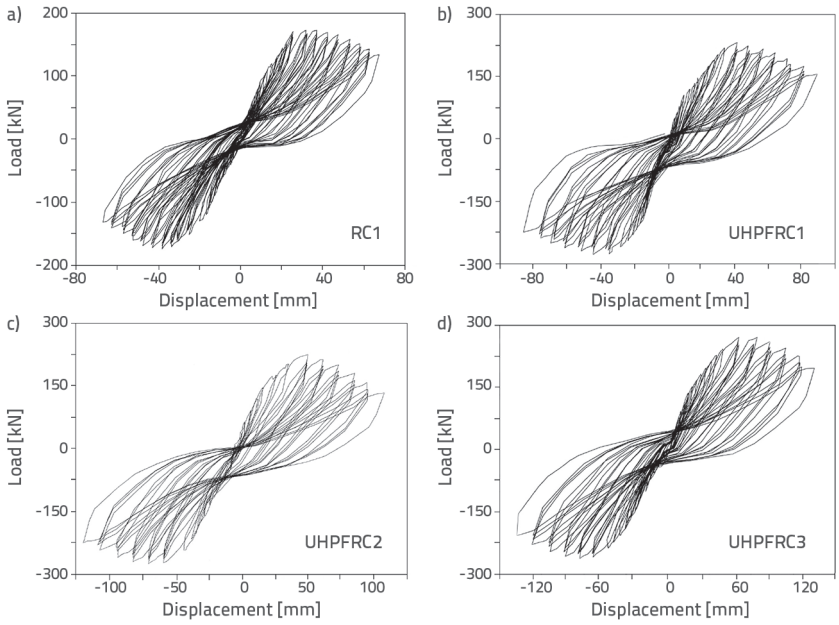

Figure 6. Load-displacement hysteresis curves

UHPFRC1 is composed of UHPFRC with ordinary-strength stirrups in the joint core. When 50 kN was loaded, multiple cracks appeared in the beam near the joint edges. The first diagonal crack appeared in the joint core when the load was increased to 150 KN. With increasing loading, the oblique crack widened and parallel cracks appeared beside it. As shown in Figure 5(b), no chipping of concrete occurred on the surface of the joint core. The failure of UHPFRC1 was attributed to the shear failure of the joint core and yielding of the longitudinal bars of the beam.

Both UHPFRC2 and UHPFRC3 were both built using UHPFRC with high-strength stirrups in the joint core and differed only in the volumetric ratio of the stirrups in the joint core. The experimental performances of UHPFRC2 and UHPFRC3 were similar to that of UHPFRC1. It can be seen from Figures 5(c) and 5(d) that their failure causes were the same as those of UHPFRC1.

3.2. Hysteretic behaviours

3.2.1. Lateral load-lateral displacement hysteresis curves

Figure 6 shows the hysteretic loops of the horizontal load and corresponding displacement at the top of the column. As shown in the figure, the four samples demonstrate similar characteristics. During the initial loading stage, the hysteresis loops are narrow. The area enclosed by the hysteresis loops increases as the load increases. After the specimens yield, the hysteresis loops exhibit inverted S-shapes.

By comparing the hysteresis curves of RC1 and UHPFRC1 in Figure 6, it can be observed that the carrying capacity and horizontal displacement of UHPFRC1 are 28.6 and 30.8 % higher than those of RC1, respectively; this can be attributed to the improved shear strength and deformation ability of the joints due to UHPFRC [29, 30]. The horizontal displacement of UHPFRC2 is 1.29 times and 0.815 times that of UHPFRC1 and UHPFRC3, respectively, and there is little difference between the bearing capacities of the three specimens (as shown in Figure 6.b, 6.c and 6.d), indicating that high-strength stirrups and increasing the stirrup ratio can improve the deformation capacity, but the influence on the bearing capacity of the joints is negligible.

3.2.2. Shear stress-shear angle hysteresis curves

The shear angles of the joint cores as dipicted in Figure 7. were calculated using the following equations (1), according [31].

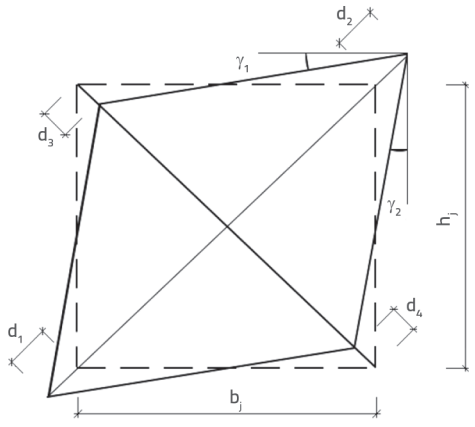

Figure 7. Shear angle of the joint core

$$\gamma = \gamma_1 + \gamma_2 = \frac{\sqrt{h_j^2 + b_j^2}}{2h_j b_j}(d_1 + d_2 + d_3 + d_4) \quad (1)$$

where γ is the shear angle of the joint core, h_j and b_j denote the height and width of the joint core, respectively, and (d_1+d_2) and (d_3+d_4) denote the changes in the lengths of the two diagonal lines.

The shear force V of the joint core as depicted in Figure 8. is expressed using the following equation (2), according [32].

$$V = \frac{P_1 L_1 + P_2 L_2}{h_{b0} - a_s}\left(1 - \frac{h_{b0} - a_s}{H_c - h_b}\right) \quad (2)$$

where P_1 and P_2 represent the forces exerted on the beam ends; L_1 (or L_2) represents the distance from the active point of P_1 (or P_2) to the column edge; H_c represents the distance between the two points of contraflexure; h_b is the beam depth; a_s is the distance between the centre point of the longitudinal compression reinforcements and the near side of the beam section; h_{b0} is the distance between the centre point of the longitudinal tensile reinforcements and the far side of the beam section.

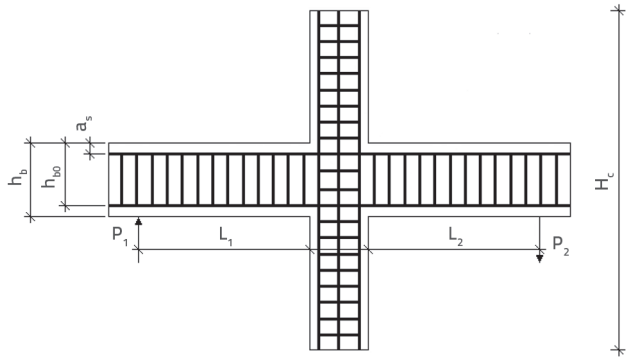

Figure 8. Calculation of shear force in the joint core

Figure 9 shows the shear stress-shear angle hysteretic curves of the joint cores. From the figure, it can be seen that the shear stress for UHPFRC1, UHPFRC2, and UHPFRC3 is similar, which is 49.3 % higher than that of RC1. This indicates that UHPFRC can significantly improve the shear capacity of joints; however, the effect of using high-strength stirrups and increasing the stirrup ratio on the shear capacity is negligible.

The shear deformation angle for UHPFRC1 increased by 66.67 % compared to RC1 (Figures 9.a and 9.b), and for UHPFRC2 and UHPFRC3 decreased by 40 and 60 % compared to UHPFRC1, respectively (Figures 9.b, 9.c and 9.d). The results show that the ductility of UHPFRC joints can be improved by increasing the stirrup ratio, and using high-strength stirrups can effectively limit the shear deformation of joints.

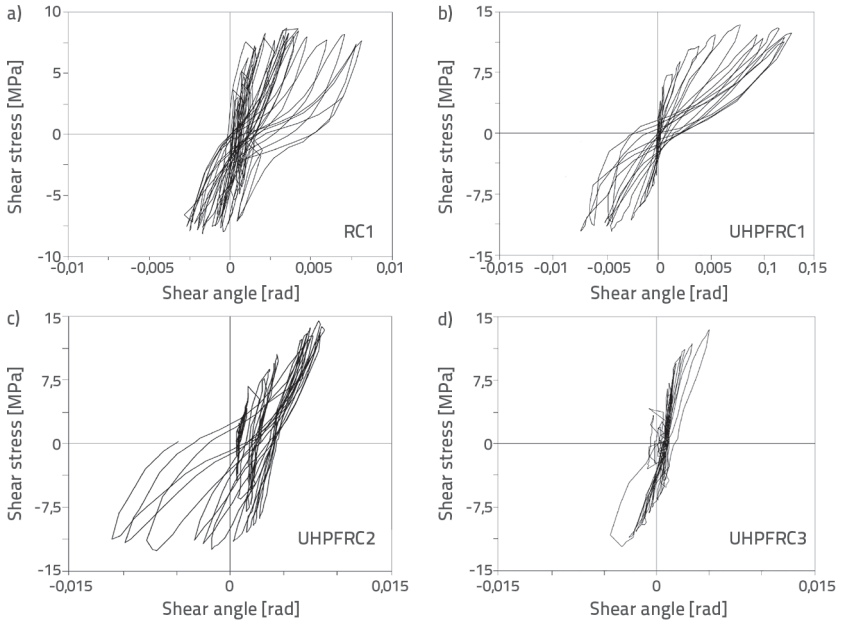

Figure 9. Shear stress-shear angle hysteresis curves

3.3. Energy dissipation

The energy-dissipating capacity of a structure or component can be quantified using the equivalent viscous damping ratio h_e [33], the larger the value of h_e is, the better the energy-dissipation capacity of the component, which can be calculated using the following equation (3), as shown in Figure 10.

$$h_e = \frac{1}{2\pi}\frac{S_{ABCD}}{S_{OBE} + S_{ODF}} \quad (3)$$

where S_{ABCD} is the area enclosed by a hysteresis loop; S_{OBE} and S_{ODF} are the areas of the triangles *OBE* and *ODF*, respectively.

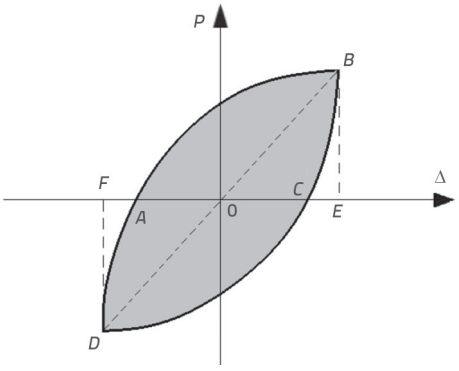

Figure 10. Calculation of the equivalent viscous damping ratio h_e

Figure 11 shows the equivalent viscous damping coefficient of each specimen, where the horizontal axis represents the ratio

of displacement to ultimate displacement. From the figure, it can be seen that at the ultimate displacement, the equivalent viscous damping ratio h_e of RC1, UHPFRC1, UHPFRC2, and UHPFRC3 are 0.165, 0.192, 0.217, and 0.234, respectively. This indicates that UHPFRC, high-strength stirrups, and higher stirrup ratios can improve the energy-dissipating capacity of the joints; that is, UHPFRC beam-column joints with high-strength stirrups have better seismic performance.

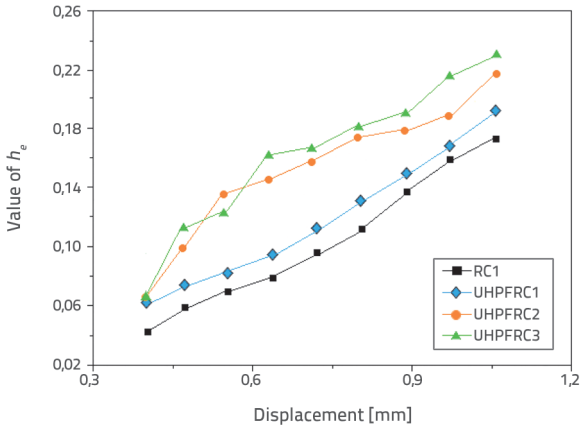

Figure 11. Comparison of values of h_e

3.4. Deformation of the bars

According to Table 4, when the diameter of the ordinary strength steel bar is 22 or 25 mm, the corresponding strain of the yield stress is 2.41 mm/m, and when the diameter of the high-strength steel bar is 5 mm, the yield strain is 5.65 mm/m. Table 6 shows the strains of the longitudinal reinforcement and stirrups in the core area when diagonal cracks occurred and the joint yielded.

When the load was low, the concrete or UHPFRC in the core area was in an elastic state and the main tensile stress was borne by the concrete. At this point, the stirrup strain was small (close to zero), or similar to a small tensile strain. When the main tensile stress in the core area exceeded the tensile strength of the concrete or UHPFRC, oblique cracks appeared along the main compressive stress trace (at approximately 45°), and the stirrup strain through the cracks increased suddenly. Concrete or UHPFRC exits work at the crack where the shear force must be borne by the stirrups that pass through the crack (forming the truss mechanism). When the stirrup strain exceeded the yield strain, significant plastic deformation occurred. Under repeated loads, the stress-strain relationship of the stirrups formed a hysteresis loop.

Table 6. Deformation of the bars

Columns	Strain gauges	X-shaped cross oblique cracks appearing		Yielding	
		Strain [mm/m]	Load [kN]	Strain [mm/m]	Load [kN]
RC1	1	1.12	110	1.67	188
	2	0.97		1.72	
	3	1.15		1.59	
	4	2.12		2.43	
	5	2.24		2.53	
UHPFRC1	1	1.14	151	1.49	290
	2	1.12		1.56	
	3	0.87		1.50	
	4	2.25		4.27	
	5	1.99		4.28	
UHPFRC2	1	0.95	154	1.53	296
	2	0.89		1.58	
	3	0.85		1.60	
	4	1.97		4.10	
	5	2.17		4.15	
UHPFRC3	1	0.99	153	1.55	289
	2	1.12		1.49	
	3	1.14		1.61	
	4	2.10		3.99	
	5	1.96		3.87	

Within the core area, the column longitudinal reinforcement was subjected to axial pressure and a small bending moment caused by the shear force transmitted by the node; therefore, its strain was usually smaller than that of the stirrups in the core area.

4. Conclusion

The mechanical properties of UHPFRC beam-column joints with high-strength stirrups were studied using quasi-static tests. The experimental results showed that UHPFRC, as an excellent substitute for concrete, combined with high-strength stirrups effectively improves the seismic performance of beam-column joints. The main conclusions are as follows.

- Failure in the joint cores of the four samples was caused by shear.
- UHPFRC not only significantly improved the bearing capacity of joints, but also increased their ductility.
- Using high-strength stirrups and increasing the stirrup ratio had little influence on the bearing capacity of the joints but improved the ductility of the joints and effectively restrained their shear deformation.
- UHPFRC beam-column joints with high-strength stirrups exhibited better energy-dissipating capacity and earthquake resistance.
- In the case of the same seismic actions, the use of UHPFRC combined with high-strength stirrups can reduce the number of stirrups by 50% compared with traditional beam-column joints, which significantly solves the construction difficulties caused by excessive reinforcement at the joints.

Acknowledgements

The authors gratefully acknowledge Dr. Tang Shougao, Tongji University, and Professor Hou Xinlu, Taiyuan University of Technology, for their invaluable support and encouragement.

REFERENCES

[1] El-Amoury, T., Ghobarab, A.J.E.S.: Seismic rehabilitation of beam-column joint using GFRP sheets, Engineering Structures, 2002, 24 (2002) 11, pp. 1397-1407, https://doi.org/10.1016/ S0141-0296(02)00081-0.

[2] Pauletta, M., Di Luca, D., Russo, G.: Exterior beam column joints-shear strength model and design formula, Engineering Structures, 94 (2015), pp. 70-81, https://doi.org/10.1016/j.engstruct.2015.03.040.

[3] Esmaeel, E., Barros, J.A., Sena-Cruz, J., Fasan, L., et al.: Retrofitting of interior RC beam-column joints using CFRP strengthened SHCC: Cast-in-place solution, Composite Structures, 122 (2015), pp. 456-467, https://doi.org/10.1016/j.compstruct.2014.12. 012.

[4] Barbhuiya, S., Choudhury, A.M.: A study of the size effect of RC beam-column connections under cyclic loading, Engineering Structures, 95 (2015), pp. 1-7, https://doi.org/10.1016/j.engstruct.2015.03.052.

[5] Chidambaram, R.S., Agarwal, P.: Seismic behaviour of hybrid fibre-reinforced cementitious composite beam-column joints, Materials & Design, 86 (2015), pp. 771-781, https://doi.org/10.1016/j.matdes.2015.07.164.

[6] Masi, A., Santarsiero, G., Lignola, G.P., Verderame, G.M.: Study of the seismic behaviour of external RC beam-column joints through experimental tests and numerical simulations, Engineering Structures, 52 (2013), pp. 207-219, https://doi.org/10.1016/j.engstruct.2013.02.023.

[7] Hadi, M.N., Tran, T. M.: Retrofitting nonseismically detailed exterior beam-column joints using concrete covers together with a CFRP jacket, Construction and Building Materials, 63 (2014), pp.161-173, https://doi.org/10.1016/j. conbuildmat.2014.04.019.

[8] Marimuthu, S., Sivasankara Pillai, G.: Experimental investigation of exterior reinforced concrete beam - column joints strengthened with hybrid FRP laminates. GRAĐEVINAR, 73 (2021) 4, pp. 365-379, https://doi.org/10.14256/JCE.2765.2019

[9] Pekgokgoz, R.K., Avcil, F.: Effect of steel fibres on reinforced concrete beam-column joints under reversed cyclic loading, GRAĐEVINAR, 73 (2021) 12, pp. 1185-1194, https://doi.org/10.14256/JCE.3092.2020

[10] Cosgun, T., Cosgun, C., Kanishka, A., Mangir, A., Sayin, B., Murat Turk, A.: Seismic load tests on exterior beam-column connections of existing RC structures, GRAĐEVINAR, 71 (2019) 12, pp. 1129-1141, https://doi.org/10.14256/JCE.2524.2018

[11] Tiwary, A.K., Singh, S., Chohan, J.S., Kumar, R., Sharma, S., Chattopadhyaya, S., Abed, F., Strepinac, M.: Behaviour of RC beam-column joints strengthened with modified reinforcement techniques, Sustainability, 14 (2022) 3, Paper 1918, https://doi.org/10.339/su14031918.

[12] Tang, L., Tian, W.H., Guan, D., Chen, Z.: Experimental study of emulative precast concrete beam-to-column connections locally reinforced by U-shaped UHPC shells, Materials, 15 (2022) 12, pp. 4066, https://doi.org/10.3390/ ma15124066.

[13] Wang, D., Ju, Y., Zheng, W., Shen, H.: Seismic behaviour and shear bearing capacity of ultra-high-performance fibre-reinforced concrete (UHPFRC) beam-column joints, Applied Sciences, 8 (2018), Paper 810, https://doi.org/10.3390/app8050810.

[14] Sarmiento, P.A., Torres, B., Ruiz, D.M., Alvarado, Y.A., Gasch, I., Machuca, A.F.: Cyclic behaviour of ultra-high performance fibre reinforced concrete beam-column joint, Structural Concrete, 20 (2019) 1, pp. 348-360, https://doi.org/10.1002/suco.201800025.

[15] Annadurai, A. Ravichandran, A.: Seismic behaviour of beam-column joint using hybrid fibre-reinforced high-strength concrete, Iranian Journal of Science and technology, 42 (2018)3, pp. 275-286, https://doi.org/10.1007/S40996-018-0100-9.

[16] Tsonos, A.D., Kalogeropoulos, G., Iakovidis, P., Bezas, M.Z., Koumtzis, M.: Seismic performance of RC beam-column joints designed according to older and modern codes: An attempt to reduce conventional reinforcement using steel fibre-reinforced concrete, Fibers, 9 (2021) 7, Paper 45, https://doi.org/10.3390/fib9070045.

[17] Nouri, A., Saghafi, M.H., Golafshar, A.: Evaluation of beam-column joints made of HPFRCC composites to reduce transverse reinforcement, Engineering Structures, 201 (2019), Paper 109826, https://doi.org/10.1016/j. engstruct.2019.109826.

[18] Wang, D., Zhao, J., Ju, Y., Shen, H., Li ,X.:. Behaviour of beam-column joints with high-performance fibre-reinforced concrete under cyclic loading, Structures, 44 (2022), pp. 171-185, https://doi.org/10.1016/j.istruc.2022.07.090.

[19] Zhang, Z.Y., Ding, R., Nie, X., Fan, J.S.: Seismic performance of a novel interior precast concrete beam-column joint using ultra-high-performance concrete, Engineering Structures, 222 (2020), Paper 111145, https://doi.org/10.1016/j.engstruct.2020.111145.

[20] Ma, F., Deng, M., Ma, Y., Lü, H., Yang, Y., Sun, H.: Experimental study on interior precast concrete beam-column connections with lap-spliced steel bars in field-cast RPC, Engineering Structures, 228 (2021), Paper111481.

[21] Xue, W., Hu, X., Song, J.: Experimental study on seismic behaviour of precast concrete beam-column joints using UHPC-based connections, Structures, 34 (2021), pp. 4867-4881.

[22] Xiong, X.Y., Xie, Y.F., Yao, G.F., Liu, J., Yan, L.Z., He, L.: Experimental study on seismic performance of precast pre-tensioned pre-stressed concrete beam-column interior joints using UHPC for connection, Materials, 15 (2022), Paper 5791, https://doi.org/10.3390/ma15165791.

[23] Shi, K., Zhang, M.Y., Tao Zhang, T., Li, P.F., Zhu, J.P., Li, L.: Seismic Performance of Steel Fiber Reinforced High-Strength Concrete Beam Column Joints, Materials, 14 (2021) 12, Paper 3235, https://doi.org/10.3390/ma14123235.

[24] Shi, K., Zhu, J.P., Li, P.F., Zhang, M.Y., Xue, R., Zhang, T.: Numerical Simulation on Seismic Behavior of Steel Fiber Reinforced Concrete Beam-Column Joints, Materials, 14 (2021) 17, Paper 4883, https://doi.org/10.3390/ma14174883.

[25] Tsonos, A.D., Kalogeropoulos, G., Iakovidis, P., Bezas, M.Z., Koumtzis, M.: Seismic performance of RC beam-column joints designed according to older and modern codes: An attempt to reduce conventional reinforcement using steel fibre reinforced concrete, Fibers, 9 (2021), Paper 45, https://doi.org/10.3390/fib9070045.

[26] Abdo, A., Mohamed, H.A., Ryad, T., Ahmed, S.: Impact of using UHPFRC in beam-column joints with different transverse reinforcement patterns, Frattura ed Integrità Strutturale, 64 (2023), pp. 11-30, https://doi.org/10.3221/IGF-ESIS.64.02.

[27] Gupta, C., Rajendran, S.C., Danie Roy, A.: Shear resistance behaviour of exterior beam-column joint with steel fibre reinforced concrete, Advances in Structural Mechanics and Applications, 19 (2022), pp. 321-335.

[28] GB 50010-2010, Code for design of concrete structure: China Architecture and Building Press, Beijing, China, 2010.

[29] Abbas, A.A., Mohsin, S.M.S., Cotsovos, D.M.: Seismic response of steel fibre reinforced concrete beam-column joints, Engineering Structures, 59 (2014) 2, pp. 261-283, https://doi.org/10.1016/j.engstruct. 2013.10.046.

[30] Said, S.H., Razak, H.A.: Structural behaviour of RC engineered cementitious composite (ECC) exterior beam-column joints under reversed cyclic loading, Construction and Build Materials, 107 (2016) 1, pp. 226-234, https://doi.org/10.1016/j.conbuildmat.2016.01.001.

[31] Dang, C.T., Dinh, N.H.: Experimental study on structural performance of RC exterior beam-column joints retrofitted by steel jacketing and haunch element under cyclic loading simulating earthquake excitation, Advances in Civil Engineering, (2017), pp. 1-11, https://doi.org/10.1155/2017/9263460.

[32] GB 50011-2010: Code for Seismic Design of Buildings, China Building Industry Press: Beijing, China, 2010.

[33] Hwang, S.J., Lee, H.J.: Analytical model for predicting shear strengths of interior reinforced concrete beam-column joints for seismic resistance, ACI Structural Journal, 96 (2000), pp. 846-857.